

# A sensitive search for CO J=1–0 emission in 4C 41.17: high-excitation molecular gas at $z=3.8$

Padeli P. Papadopoulos<sup>1</sup>, Thomas R. Greve<sup>2</sup>, R. J. Ivison<sup>3,4</sup>, and Carlos De Breuck<sup>5</sup>

<sup>1</sup> Institut für Astronomie, ETH, 8093 Zürich, Switzerland

<sup>2</sup> California Institute of Technology, Pasadena, CA 91125, USA

<sup>3</sup> Astronomy Technology Centre, Royal Observatory, Blackford Hill, Edinburgh EH9 3HJ, UK

<sup>4</sup> Institute for Astronomy, University of Edinburgh, Blackford Hill, Edinburgh EH9 3HJ, UK

<sup>5</sup> European Southern Observatory, Karl Schwarzschild Straße 2, D-85748 Garching, Germany

Received / Accepted

**Abstract.** We report sensitive imaging observations of the CO J=1–0 line emission in the powerful high-redshift radio galaxy 4C 41.17 ( $z = 3.8$ ) with the NRAO Very Large Array (VLA), conducted in order to detect the large concomitant H<sub>2</sub> gas reservoir recently unveiled in this system by De Breuck et al. (2005) via the emission of the high excitation J=4–3 line. Our observations fail to detect the J=1–0 line but yield sensitive lower limits on the  $R_{43} = (4 - 3)/(1 - 0)$  brightness temperature ratio of  $R_{43} \sim 0.55 - \gtrsim 1.0$  for the *bulk* of the H<sub>2</sub> gas mass. Such high ratios are typical of the high-excitation molecular gas phase “fueling” the star formation in local starbursts, but quite unlike these objects, much of the molecular gas in 4C 41.17 seems to be in such a state, and thus participating in the observed starburst episode. The widely observed and unique association of highly excited molecular gas with star forming sites allows CO line emission with large (high-J)/(low-J) intensity ratios to serve as an excellent “marker” of the spatial distribution of star formation in distant dust-obscured starbursts, unaffected by extinction.

**Key words.** Galaxies: individual (4C41.17) – galaxies: active – galaxies: starbursts – ISM: molecules

## 1. Introduction

The powerful radio galaxy 4C41.17 at  $z = 3.8$  with a far-infrared (FIR) luminosity of  $L_{\text{FIR}} \sim 10^{13} L_{\odot}$  is the site of an enormous starburst event in the distant Universe (e.g. Eales et al., 1993; Graham et al., 1994), an interpretation put forth since its discovery (Chambers et al., 1990). This view received additional support from the discovery of a large dust mass (Chini & Krügel, 1994; Dunlop et al., 1994), and its concomitant molecular gas reservoir with  $M(\text{H}_2) \sim 5 \times 10^{10} M_{\odot}$  (De Breuck et al., 2005), which presumably fuels the star formation. This follows the path of similar discoveries made in the last decade, uncovering vast molecular gas masses residing in a variety of high-redshift objects. These include QSOs (Barvainis et al., 2004; Omont et al., 1996; Ohta et al., 1996), submm-selected galaxies (Frayser et al., 1998; Neri et al., 2003), Ly-break galaxies (Baker et al., 2004) and powerful radio galaxies Klammer et al. (2005). The highest redshift at which CO has been detected stands now at  $z = 6.42$ , when the Universe was less than a Gyr old (Walter et al., 2003; Bertoldi et al., 2003).

Aside from the intrinsic interest of studying the molecular gas in distant powerful radio galaxies, the likely formation

sites of present-day giant ellipticals and their surrounding clusters (e.g. Pentericci et al., 1997; Archibald et al., 2001), the case of 4C41.17 is special since it was the first *non-lensed* high-redshift object for which dedicated, sensitive observations were conducted to detect its molecular gas mass (Ivison et al., 1996; Barvainis & Antonucci, 1996). Observations of CO J=1–0 are of particular importance since they provide the least excitation-biased method of tracing metal-rich H<sub>2</sub> gas ( $E_1/k_B \sim 5.5$  K,  $n_{\text{cr}} \sim 400$  cm<sup>-3</sup>), while most of the reported searches/detections of molecular gas in high-redshift objects use CO J+1→J, J+1≥3 and usually J = 4–3 or higher transitions (e.g. Evans et al., 1996; van Ojik et al., 1997; Downes et al., 1999). These transitions, with their much higher critical densities and energy levels (e.g. for CO 4–3:  $n_{\text{cr}} \sim 2 \times 10^4$  cm<sup>-3</sup>,  $E_4/k_B \sim 55$  K) trace much warmer and denser gas, and thus may not reveal the distribution of the bulk of the molecular gas.

Evidence for molecular gas, sub-thermally excited over large scales, has emerged for a few objects at high redshifts (e.g. Papadopoulos & Ivison, 2002; Greve et al., 2003) and for this reason we followed up the recent detection of CO J = 4–3 in 4C41.17 with sensitive observations of the J = 1–0 transition. At  $z = 3.8$  the latter is redshifted to 24 GHz and becomes

Send offprint requests to: Padeli P. Papadopoulos, e-mail: papadop@phys.ethz.ch

accessible to the K-band receivers of the VLA.<sup>1</sup> Our sensitive observations, which unlike past efforts had the advantage of knowing the line center from the detection of CO J = 4–3, do not detect any J = 1–0 emission but the lower limits they set on the  $R_{43} = (4 - 3)/(1 - 0)$  line ratio imply a high excitation for the bulk of the molecular gas. This suggests that, unlike local counterparts, most of the molecular gas reservoir in this distant galaxy participates in the observed starburst event. Throughout this work we assume  $H_0 = 75 \text{ km s}^{-1} \text{ Mpc}^{-1}$  and  $q_0 = 1/2$ .

## 2. Observations

The observations of 4C41.17 were conducted with the VLA in its D configuration with four ~8-hr tracks obtained during 2004 August 12–22 UT and a phase-tracking center at: RA (J2000) =  $06^{\text{h}} 50^{\text{m}} 52^{\text{s}}.150$  and Dec (J2000) =  $41^{\circ} 30' 30''.801$ . The CO J = 1–0 line ( $\nu_{\text{rest}} = 115.2712 \text{ GHz}$ ) at the redshift  $z = 3.7978$  of the radio galaxy (centered on its CO 4–3 emission; De Breuck et al., 2005) shifts to  $\nu_{\text{obs}} = 24.0258 \text{ GHz}$ , accessible to the VLA’s K-band receivers. Aiming solely at the detection of line emission rather than obtaining information about the velocity distribution of the molecular gas, we used the continuum correlator mode with one IF pair (left and right circular polarization) tuned to observe the line+continuum while the other one simultaneously observed the adjacent continuum. At 24 GHz the effective IF bandwidth,  $\Delta\nu_{\text{IF}} = 45 \text{ MHz}$ , corresponds to  $\Delta V_{\text{IF}} \sim 560 \text{ km s}^{-1}$ . The wide velocity range ( $\sim 1000 \text{ km s}^{-1}$ ) revealed by the CO J = 4–3 observations ensures no sensitivity loss due to velocity dilution of the J = 1–0 line within the IF bands. Two separate tunings were necessary (and were equally distributed per track) to observe the entire expected line width. These [on-line, continuum] tunings, optimized to observe the ‘blue’ and the ‘red’ velocity components of the CO J = 4–3 emission, were: [24.0649, 24.1649] GHz and [24.0351, 23.9351] GHz, corresponding to [–490, –1735]  $\text{km s}^{-1}$  and [–115, +1130]  $\text{km s}^{-1}$  velocity offsets relative to  $\nu_{\text{obs}}(z)$ .

During our observing sessions the system temperatures were  $T_{\text{sys}} \sim (70 - 90) \text{ K}$ , and a fast-switching technique was used (Carilli & Holdaway, 1999), recording data every 5 sec (integration time per visibility) with 20 sec spent on the compact calibrator 06465+44513 and 150 sec on source; the typical slewing time to the calibrator,  $3.5^{\circ}$  away, was 20 sec. This ensured very good amplitude and phase calibration with a resulting phase  $|\phi_{\text{rms}}| \lesssim 25^{\circ}$  for most of the time. The latter was estimated from the residual phases of our amplitude/phase calibrator after applying antenna gain solutions smoothed to  $\sim 3 \times \Delta t_{\text{cal}}$  ( $\Delta t_{\text{cal}} \sim 3.2 \text{ min}$ : interval between successive observations of the calibrator). The flux density scale was set using 3C 286 (2.59 Jy) and 0713+438 (0.55 Jy). The resulting bootstrapped flux of 06465+44513, used for the final amplitude/phase calibration of the data, was  $S(24 \text{ GHz}) = 3.15 \text{ Jy}$  (averaged over all four days), and carries an uncertainty of  $\sim 15\%$ .

<sup>1</sup> The National Radio Astronomy Observatory is a facility of the National Science Foundation operated under cooperative agreement by Associated Universities, Inc.

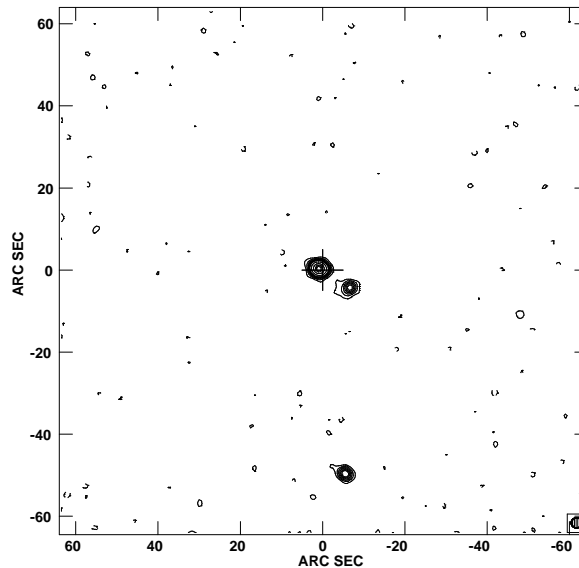


**Fig. 1.** Radio continuum map of 4C41.17 at 24 GHz resulting from imaging all the  $uv$  datasets (see text). Robust weighting was applied (with `ROBUST = 0`) and `CLEAN` was employed, converging to a total flux  $S_{\text{CL}} = 4.88 \text{ mJy}$ . The map was then convolved to circular synthesized beam of  $\text{FWHM}=2.5''$  shown at the bottom right. The contours are at  $(-3, 3, 6, 9, 12, 15, 18, 30, 50, 70, 80) \times \sigma$ , with  $\sigma = 28 \mu\text{Jy beam}^{-1}$ . The cross marks the position of the radio core, RA (J2000):  $06 50 52.15$ , Dec (J2000):  $+41 30 30.80$  (Carilli et al., 1994), which is also the phase tracking center of the observations presented.

### 2.1. Data reduction: the search for CO J = 1–0 line emission

The measured visibilities were carefully edited and calibrated using standard techniques described in the NRAO *AIPS* Cookbook and then Fourier transformed (using the task `imagr`) to produce images. `CLEANing` was applied to produce the final (deconvolved) images of the emission of 4C41.17 at 24 GHz. In all our naturally-weighted maps the measured r.m.s. noise was close to the theoretical value expected from the number of the visibilities imaged, the system temperatures during our observations, two IFs per frequency and an assumed antenna aperture efficiency of  $\eta_a = 0.40$  at  $24 \text{ GHz}$ <sup>2</sup>. A map of the entire field of view of the primary beam ( $\sim 2'$ ), using all the data is shown in Fig. 1. The flux densities measured for the core and its SW feature are:  $S_{\text{core}} = (2.97 \pm 0.45) \text{ mJy}$  and  $S_{\text{SW}} = (0.73 \pm 0.12) \text{ mJy}$ , in good agreement with those reported for these components by Ivison et al. (1996). The SW feature corresponds to feature ‘A’ in low-frequency maps (Chambers et al., 1990; Carilli et al., 1994) and is dominated by optically thin synchrotron emission from the radio lobe, with a steep spectral index  $\alpha = -1.7$  ( $S_\nu \propto \nu^\alpha$ ) (Ivison et al., 1996). For the emission feature at  $\Delta\theta \sim -50''$  to the South (also

<sup>2</sup> VLA Observational Status Summary 2004

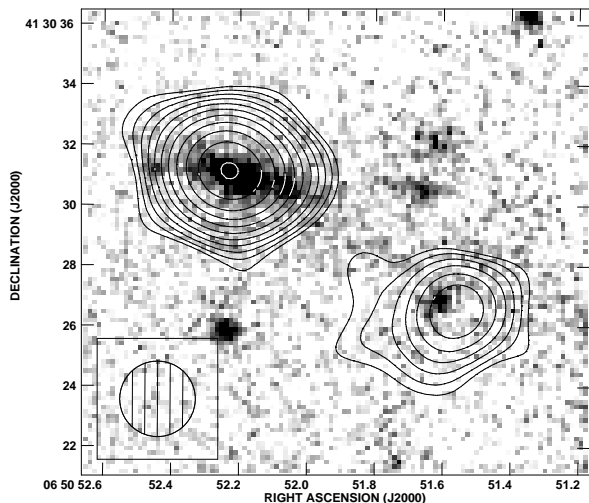


**Fig. 2.** Radio continuum map of 4C 41.17 at 24 GHz (contours) overlaid on the 2.15- $\mu\text{m}$  image obtained at the Keck Observatory (Graham et al. 1994). The contour levels are (3, 4.25, 6, 8.5, 12, 17, 24, 34, 48, 68, 96)  $\times\sigma$ , with  $\sigma=26 \mu\text{Jy beam}^{-1}$ .

seen in the maps of Carilli et al. 1994) we find a probability of it due to chance of  $P(\Delta\theta) \sim 0.25$ , thus the association is not significant.<sup>3</sup>

An overlay of our new 24-GHz map with those obtained at 1.4 and 5 GHz (Carilli et al., 1994) reveals excellent correspondence of the emission features across all three wavelengths, a testimony to the good phase calibration at 24 GHz resulting from our fast-switching scheme. A deep  $K_S$ -band (2.15  $\mu\text{m}$ ) image shows a faint feature just upstream from the SW radio lobe A (see Fig. 2). At a redshift of  $z = 3.8$ , 2.15  $\mu\text{m}$  corresponds to rest-frame  $B$ -band, expected to be dominated by young stars. This is especially true since the  $K_S$ -band is free of emission-line contamination, and the scattered AGN light is expected to be negligible  $\sim 35$  kpc from the radio core position. If this component is indeed at the redshift of 4C41.17, it would indicate a second locus of jet-induced star formation in this distant radio galaxy (Dey et al., 1997; Bicknell et al., 2000).

We searched for CO J = 1–0 emission by comparing the images “on” and “off” the expected line for the two different frequency settings covering its velocity range (as revealed by the CO J = 4–3 emission). We did not find any significant excess flux density in the maps “on” with respect to those “off” the line, within the noise levels achieved, while the total CLEANed flux density of the radio galaxy is similar for these maps and for both frequency settings. We produced line-only maps using the *ATPS* task *uvsub*: the *clean* components of the continuum maps were Fourier transformed back to the visibility plane, re-sampled by the *uv* sampling function (identical for the simultaneously obtained on-line and off-line datasets), then

<sup>3</sup> We estimate  $P(\Delta\theta)$  following the method outlined by Downes et al. (1986) and the 1.4-GHz number counts reported by Hopkins (2003) after we extrapolate a flux of  $S_{1.4\text{GHz}} = 5$  mJy for our source (assuming a spectral index of  $\alpha = -0.7$  between 1.4 and 24 GHz).

subtracted from the (line + continuum) visibilities. The resulting continuum-free visibilities were then Fourier transformed (without CLEANing) to produce naturally weighted (for maximum sensitivity) images (Figs 3 and 4). Significantly tapered images from these visibilities were also made to investigate the presence of any extended, low-brightness, line emission but no evidence of this was found.

Tantalizingly, in the frequency setting covering the “blue” profile of the CO J = 4–3 line some faint emission can be seen in the line map, located between the two radio continuum components (Fig. 3). However, this is not statistically significant, especially since the noise measured within the area containing the radio galaxy (and where the *clean* components of its continuum are derived) is somewhat higher than in the rest of the image, namely  $\sigma_{\text{eff}} = 65 \mu\text{Jy beam}^{-1}$ . This is expected since subtracting the noisy *clean* components,  $N_{\text{CL}}$ , defining the radio continuum emission will add noise to that part of the resulting continuum-free image ( $\sigma_{\text{eff}} < \sqrt{2}\sigma \sim 80 \mu\text{Jy beam}^{-1}$ , simply because  $N_{\text{CL}} < N_{\text{pixels}}$ ). We use  $\sigma_{\text{eff}}$  to express the 1- $\sigma$  upper limit of the velocity-integrated CO J = 1–0 line from

$$\Delta S_{1-0} = \int_{\Delta v} \delta S_v dV = c \left( \frac{\Delta v_{\text{IF}}}{v_{\text{obs}}} \right) \sqrt{N_b} \sigma_{\text{eff}}, \quad (1)$$

where  $N_b$  is the number of beams associated with the putative CO-emitting area. A single IF covers most of each of the detected J = 4–3 “blue” and “red” velocity components, with  $\Delta S_{1-0} = 0.035$  Jy km s<sup>-1</sup> (point source sensitivity,  $N_b = 1$ ), and a corresponding limit on the J=1–0 luminosity per component of  $L_{\text{co}} \sim 10^{10}$  K km s<sup>-1</sup> pc<sup>2</sup>. The corresponding lower limit for the velocity/area-averaged  $R_{43}$  line ratios can be found from

$$R_{43} = \frac{\langle T_b(4-3) \rangle}{\langle T_b(1-0) \rangle} = \left( \frac{v_{10}}{v_{43}} \right)^2 \frac{S_{4-3}}{S_{1-0}}. \quad (2)$$

The CO J = 4–3 emitting regions are unresolved by the  $\theta_{\text{HPBW}} \sim 6''$  of the Plateau de Bure Interferometer, thus  $N_b(\text{max}) \sim 3.5$ . Using the numbers reported by De Breuck et al. for  $S_{4-3}$ , and considering a 2- $\sigma$  upper limit for the J = 1–0 emission, with  $N_b = 3.5$ , yields  $R_{43}^{(b)} \gtrsim 0.30$  and  $R_{43}^{(r)} \gtrsim 0.55$  for the “blue” and “red” component, the latter containing most of the H<sub>2</sub> gas mass in this system. For a CO emitting region smaller than our resolution limit of  $\sim 3''$ ,  $N_b = 1$  and these limits become  $R_{43}^{(b)} \gtrsim 0.55$  and  $R_{43}^{(r)} \gtrsim 1$ . These are the highest minimum values compatible with the sensitivity of our measurements, and the most likely ones since in this object  $\theta_{\text{co}} \lesssim 0.3''$  (De Breuck et al., 2005), and are adopted in all our subsequent analysis.

### 3. Discussion

The models of the molecular gas physical conditions constrained by single or even multiple line ratios (*e.g.* Aalto et al., 1995) contain significant degeneracies, but for modest-to-high values of CO line ratios with large J-level differences (and thus difference between  $n_{\text{cr}}$  and  $E_{\text{upper}}/k_B$ ) these are significantly reduced. The CO J = 4–3 transition in particular marks a broad excitation turnover beyond which line flux densities and thus the line ratios  $R_{J+1J}$  ( $J+1 \geq 4$ ) become highly dependent on

the ambient gas conditions and can vary widely (Nieten et al., 1999; Carilli et al., 2002). Moreover, because of the difficulty of routine observations at  $\nu \gtrsim \nu_{43} \sim 461$  GHz through the Earth’s atmosphere, ratios like  $R_{43}$  are sensitive probes of gas excitation that are rarely available in the local Universe.

The lower limit of  $R_{43} \geq 0.55$  of the “blue” emission component in 4C 41.17 is within the range of the  $R_{43}$  values measured in another powerful radio galaxy, 4C 60.07 at  $z \sim 3.8$  (Greve et al., 2004), and suggests highly excited gas. By comparison, the *globally averaged* CO emission for the Galaxy measured by *COBE*, yields  $R_{43} \sim 0.10 - 0.17$ , indicative of a quiescent gas phase (Fixsen et al., 1999). A single-phase Large Velocity Gradient (LVG) model, restricted by setting  $T_k = T_{\text{dust}} \sim (50 - 60)$  K (De Breuck et al., 2005), yields  $n(\text{H}_2) \gtrsim 10^3 \text{ cm}^{-3}$  for most solutions, which is on the upper end of the *mean* densities of Giant Molecular Clouds in the Galactic disk ( $\sim (10^2 - 10^3) \text{ cm}^{-3}$ ). If an ensemble of virialized clouds is assumed, the average cloud density and its associated velocity gradient are no longer independent but related as

$$\left(\frac{dV}{dR}\right)_{\text{VIR}} \approx 0.65\alpha^{1/2} \left(\frac{n}{10^3 \text{ cm}^{-3}}\right)^{1/2} \text{ km s}^{-1} \text{ pc}^{-1}, \quad (3)$$

where  $\alpha = 0.5 - 2.5$  depends primarily on the cloud density profile (Papadopoulos & Seaquist, 1999). For  $dV/dR = (dV/dR)_{\text{VIR}}$  (and an abundance  $[^{12}\text{CO}/\text{H}_2] \sim 10^{-4}$ ), the LVG solutions compatible with  $R_{43} \gtrsim 0.55$  have  $T_k \sim (40 - 50)$  K for densities of  $\sim (1 - 3) \times 10^3 \text{ cm}^{-3}$ . However, in starburst environments highly non-virial motions have been deduced (Downes & Solomon, 1998) and thus LVG solution constraints based on known dust temperatures are better than assumptions of virialized  $^{12}\text{CO}$ -emitting clouds. For the “red” kinematic component, with  $R_{43} \gtrsim 1$ , our models yield  $n(\text{H}_2) \gtrsim 10^4 \text{ cm}^{-3}$  (for  $T_k \sim (50 - 60)$  K), typical for  $\text{H}_2$  gas in star-forming regions. The solutions compatible with  $R_{43} > 1$  and  $T_k \sim (50 - 60)$  K typically have moderate CO J=1-0 optical depths ( $\tau_{10} \sim 1 - 2$ ), a condition encountered often for the warm and turbulent molecular gas in starburst environments (Aalto et al., 1995).

### 3.1. The dominance of high-excitation gas in 4C 41.17

One-phase LVG modeling of CO line ratios encompassing entire galaxies (the case for most high redshift CO line detections), can yield only indicative results regarding which conditions are prevalent in their large molecular gas reservoirs. A different way to determine the relative prevalence of a highly-excited, starburst-fueling, gas phase is to make use of its well-established characteristics (and typical CO line ratios) along with those of a quiescent, star-formation-idle one. These two phases have been extensively studied in the local Universe where observations of several molecular and atomic lines, as well as a high spatial resolution, allow their detailed and realistic modeling (see Papadopoulos, Thi, & Viti 2004 for a review).

In the local Universe, the unique association of  $R_{J+1J} \sim 1$ ,  $J + 1 \leq 4$  ratios (typical of high-excitation molecular gas) with sites of vigorous star formation has become apparent since the first extragalactic detection of CO J=4-3 emission

by Güsten et al. (1996) towards the star-forming regions of the nearby archetypal starburst galaxies M82, NGC 253 and IC 342 where typical (4-3)/(2-1) CO line ratios of  $R_{43/21} \gtrsim 0.5 - 0.8$  were measured. For M82 this was confirmed by much more detailed studies (Mao et al., 2000), while a recent study demonstrated the existence of an additional massive low-excitation gas phase extending much further ( $\sim 3$  kpc) than the starburst-related gas residing in its inner 500 pc (Weiß et al., 2005).

For starbursts at high redshifts, the distribution of star forming regions is one of the crucial aspects that can distinguish between scaled-up (in terms of star formation rate) versions of local starburst galaxies (usually with compact star-forming regions) and very different, galaxy-wide events. Extended CO line emission with large (high-J)/(low-J) intensity ratios can be an excellent “marker” of the spatial distribution of star formation in distant dust-obscured starbursts, *unaffected by extinction*. In the case of 4C 41.17 the CO J=4-3 emission is unresolved, but the distribution of a high-excitation, star-forming, gas phase and its concomitant starburst relative to the total CO-emitting area can be constrained from our limit on the global  $R_{43}$  ratio. Indeed, for the large velocity gradients characterizing molecular clouds (thus no significant radiative “shadowing” between different gas phases) it is

$$R_{43} = \frac{R_{43}^{(l)} + \rho_{\text{hl}} f_{\text{hl}} R_{43}^{(h)}}{1 + \rho_{\text{hl}} f_{\text{hl}}}, \quad (4)$$

where  $R_{43}^{(h)}$  and  $R_{43}^{(l)}$  are the (4-3)/(1-0) ratios of the velocity/area-averaged, CO emission of the high-excitation and low-excitation molecular gas phase,  $f_{\text{hl}} = \Omega_{\text{h}}/\Omega_{\text{l}}$  the ratio of their emitting areas, and  $\rho_{\text{hl}} = [J(T_k^{(h)}) - J(T_{\text{bg}})]/[J(T_k^{(c)}) - J(T_{\text{bg}})]$  (for optically thick and thermalized J=1-0 transition for both phases), where  $J(T) = h\nu/k_B(e^{h\nu/k_B T} - 1)^{-1}$  ( $\nu = \nu_{10} \sim 115$  GHz) and  $T_{\text{bg}} = (1 + z)T_{\text{cmb}} \sim 13$  K is the CMB temperature at  $z \sim 3.8$ . Setting  $R_{43}^{(h)} = 1$  (typical for the high-excitation, star-forming gas phase e.g. Weiß et al., 2005 and references therein), and  $R_{43}^{(l)} = 0.15$  for the quiescent and star-formation-idle one (Fixsen et al., 1999), the lower limit  $R_{43} \sim 0.55$  corresponds to  $\rho_{\text{hl}} f_{\text{hl}} \sim 0.9$ . For typical temperatures usually associated with these gas phases:  $T_k^{(l)} \sim 20$  K and  $T_k^{(h)} \sim 60$  K, it is  $f_{\text{hl}} \sim 0.13$ . The latter amounts to  $f_{\text{h}} = f_{\text{hl}}/(1 + f_{\text{hl}}) \sim 0.10$  of the total CO-emitting region occupied by the high-excitation gas phase and its concomitant starburst (by comparison in M82:  $f_{\text{h}} \sim 0.03$ ). A maximum value for  $f_{\text{hl}}$  and  $f_{\text{h}}$  can be found by setting  $T_k^{(h)} \sim T_k^{(w)}$  (thus  $\rho_{\text{hl}} \sim 1$ ), i.e. the difference in the  $R_{43}$  ratio (and the excitation state of J=4-3) between the two gas phases is solely due to a difference in densities, yielding  $f_{\text{hl}} \sim 0.9$  and  $f_{\text{h}} \sim 0.47$ . In practice both temperature and density effects play a role and the true  $f_{\text{h}}$  will lie between the aforementioned estimated values. These are applicable to the “blue” component; in the “red” component, which hosts the radio-loud AGN, the  $R_{43} \gtrsim 1$  limit implies a high-excitation gas phase that fully dominates the CO emission.

## 4. Conclusions

We report sensitive new observations of the CO J = 1–0 transition in the distant, powerful radio galaxy 4C 41.17 at  $z = 3.8$  using the NRAO Very Large Array. Our results can be summarized as follows:

1. The CO J=1–0 line emission remains undetected but the new sensitive upper limit and the detected J=4–3 line yields a brightness temperature ratio of  $R_{43} \sim 0.55 - \gtrsim 1$  for the *bulk* of its H<sub>2</sub> gas reservoir. This ratio is  $\sim 3-6$  times higher than the one in quiescent environments of the Galaxy, and is typical of starburst environments.
2. Single-phase Large Velocity Gradient models, under the restriction of  $T_k = T_{\text{dust}}$ , yield  $n(\text{H}_2) \sim (10^3 - \gtrsim 10^4) \text{ cm}^{-3}$ , more typical of the high-excitation gas “fueling” local starbursts rather than a more diffuse, low-excitation, phase.
3. Assuming the molecular gas reservoir to be segregated between a high-excitation star-forming, and a quiescent star-forming-idle phase, with  $R_{43}$  ratios and gas temperatures typical for the local Universe, we find the former to occupy at least  $\sim 10\%$  and up to  $\sim 100\%$  of the total CO emitting area. This is much higher than what is found in local starbursts like M 82, and equivalently demonstrates the predominance of a high-excitation gas phase fueling an extreme star formation event in this distant powerful radio galaxy.

*Acknowledgements.* We would like to thank James Graham and Wil van Breugel for providing us with the  $2.2 \mu\text{m}$  image of 4C 41.17. We are grateful to the anonymous referee for helping us to significantly improve the original manuscript.

## References

- Aalto S., Booth R.S., Black J.H., Johansson L.E.B., 1995, *A&A*, 300, 369
- Archibald E.N. et al., 2001, *MNRAS*, 323, 417
- Baker A.J., Tacconi L.J., Genzel R., Lehnert M.D., Lutz D., 2004, *ApJ*, 604, 125
- Barvainis R., Tacconi L., Antonucci R., Alloin D., Coleman, P., 1994, *Nature*, 371, 586
- Barvainis R., Antonucci R., 1996, *PASP*, 108, 187
- Bertoldi F. et al., 2003, *A&A*, 409, L47
- Bicknell G.V. et al., 2000, *ApJ*, 540, 678
- Carilli C.L., Owen F.N., Harris D.E., 1994, *AJ*, 107, 480
- Carilli C.L. & Holdaway M.A., 1999, *Radio Science*, 34, 817
- Carilli C.L. et al., 2002a, *AJ*, 123, 1838
- Carilli C.L. et al., 2002b, *ApJ*, 575, 145
- Chambers K.C., Miley G.K., van Breugel W.J.M., 1990, *ApJ*, 363, 21
- Chini R., Krügel E., 1994, *A&A*, 288, L33
- De Breuck C., Downes D., Neri R., van Breugel W., Reuland M., Omont A., Ivison R., 2005, *A&A*, 430, L1
- Devereux N., Taniguchi Y., Sanders D.B., Nakai N., Young J.S., 1994, *AJ*, 107, 2006
- Dey A., van Breugel W., Vacca W.D., Antonucci R., 1997, *ApJ*, 490, 698
- Downes A.J.B., Peacock J.A., Savage A., Carrie D.R., 1986, *MNRAS*, 218, 31
- Downes D., & Solomon P.M., 1998, *ApJ*, 507, 615
- Downes D., Neri R., Wiklind T., Wilner D.J., Shaver P.A., 1999, *ApJ*, 513, L1
- Dunlop J.S., Hughes D.H., Rawlings S., Eales S.A., Ward M.J., 1994, *Nature*, 379, 347
- Eales S.A., Rawlings S., 1993, *ApJ*, 411, 67
- Evans A.S., Sanders D.B., Mazzarella J.M., Solomon P.M., Downes D., Kramer C., Radford S.J.E., 1996, *ApJ*, 457, 658
- Fixsen D. J., Bennett C. L., & Mather J. C. 1999, *ApJ*, 526, 207
- Frazer D.T. et al., 1998, *ApJ*, 506, L7
- Graham J.R. et al., 1994, *ApJ*, 420, L5
- Greve T.R., Ivison R.J., Papadopoulos P.P., 2003, *ApJ*, 599, 839
- Greve T.R., Ivison R.J., Papadopoulos P.P., 2004, *A&A*, 419, 99
- Güsten R., Serabyn E., Kasemann C., Schinckel A., Schneider G., Schulz E., & Young K., 1996, *ApJ*, 402, 537
- Hopkins A.M., PhD Thesis, University of Sydney
- Ivison R.J., Papadopoulos P., Seaquist E.R., Eales S.A., 1996, *MNRAS*, 278, 669
- Klamer I.J., Ekers R.D., Sadler E.M., Weiss A., Hunstead R.W., De Breuck C., 2005, *ApJ*, 621, 1
- Mao R.Q., Henkel C., Schulz A., Zielinsky M., Mauersberger R., Störzer H., Wilson T.L., & Gensheimer P., 2000, *A&A*, 433, 450
- Neri R. et al., 2003, *ApJ*, 597, L113
- Nieten Ch., Dumke M., Beck R., Wielebinski R., 1999, *A&A*, 347, L5
- Omont A., Petitjean P., Guilloteau S., McMahon R.G., Solomon, P.M., Pecontal E., 1996, *Nature*, 382, 428
- Ohta K., Yamada T., Nakanishi K., Kohno K., Akiyama M., Kawabe R., 1996, *Nature*, 382, 426
- Papadopoulos P.P., & Seaquist E.R., 1999, *ApJ*, 516, 114
- Papadopoulos P. P., Ivison R.J., 2002, *ApJ*, 564, L9
- Papadopoulos P. P., Thi W.-F., & Viti S., 2004, *MNRAS*, 351, 147
- Pentericci L., Röttgering H.J.A., Miley G.K., Carilli C.L., McCarthy P., 1997, *A&A*, 326, 580
- van Ojik R. et al., 1997, *A&A*, 321, 389
- Walter F. et al., 2003, *Nature*, 424, 406
- Walter F. et al., 2004, *ApJ*, 615, L17
- Weiss A., Walter F., & Scoville N. Z. 2005, *A&A*, 438, 533
- Wielebinski R., Dumke M., Nieten Ch., 1999, *A&A*, 347, 634

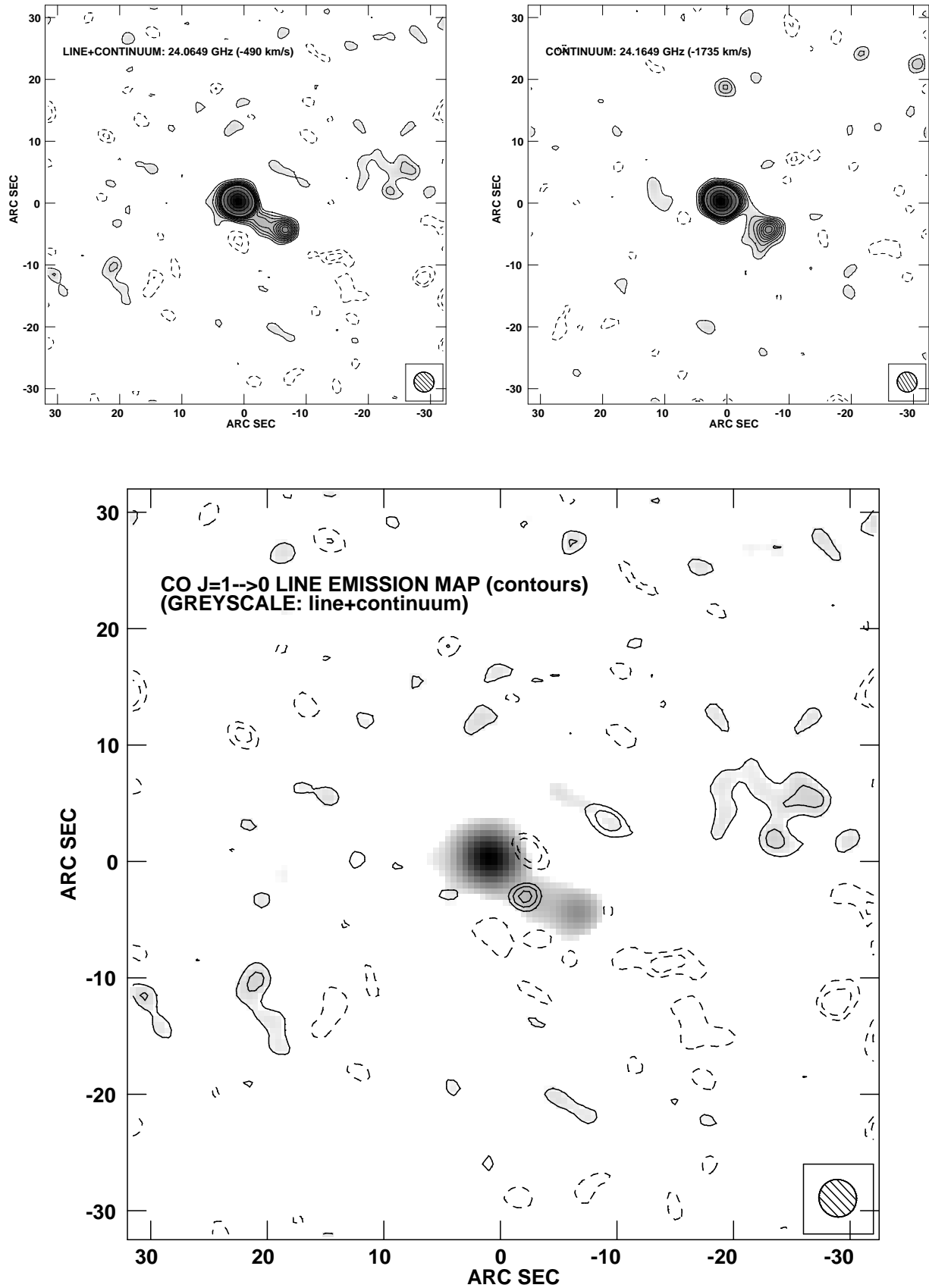


**Fig. 3.** Naturally-weighted maps of (“blue” line)+continuum (top left), continuum (top right), and line only (bottom) emission (see text). Contours:  $(-3, -2, 2, 3, 4, 5, 6, 7, 8, 9, 10, 15, 25, 35, 45, 55, 65, 75, 85) \times \sigma$  ( $\sigma = 55 \mu\text{Jy beam}^{-1}$ ). The restoring beam is  $3.27'' \times 3.16''$  and is shown at the bottom right corner (CLEAN was not applied on the continuum-free map).

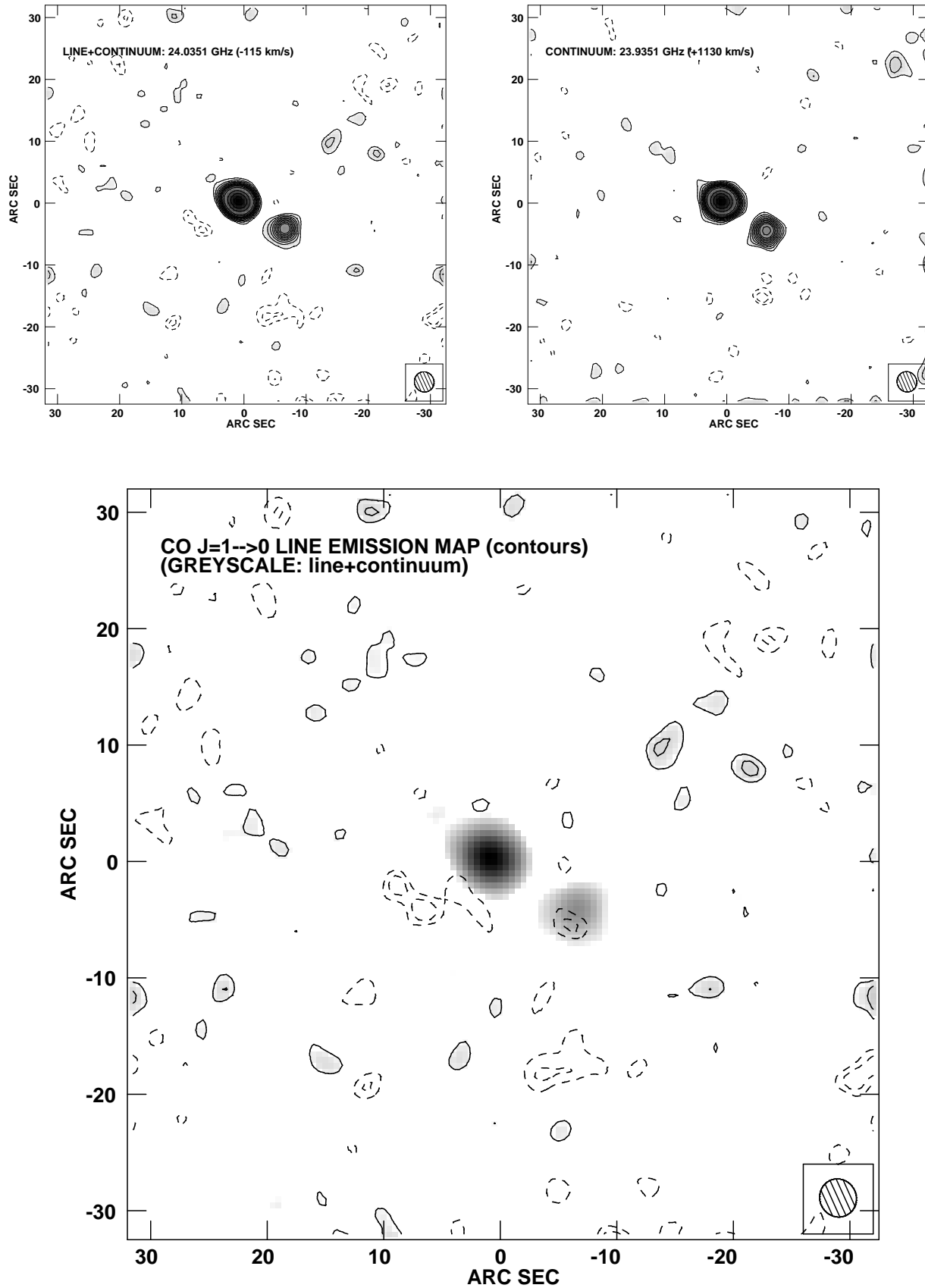


**Fig. 4.** Naturally-weighted maps of (“red” line)+continuum (top left), continuum (top right), and line only (bottom) emission (see text). Contours:  $(-3, -2, 2, 3, 4, 5, 6, 7, 8, 9, 10, 12, 15, 25, 35, 45, 55, 65, 75, 85) \times \sigma$  ( $\sigma = 55 \mu\text{Jy beam}^{-1}$ ). The restoring beam is  $3.31'' \times 3.13''$  and is shown at the bottom right corner (CLEAN was not applied on the continuum-free map).